



Carbonate Deposition, Climate Stability, and Neoproterozoic Ice Ages

Andy J. Ridgwell, *et al.*
Science **302**, 859 (2003);
DOI: 10.1126/science.1088342

The following resources related to this article are available online at www.sciencemag.org (this information is current as of May 16, 2007):

Updated information and services, including high-resolution figures, can be found in the online version of this article at:

<http://www.sciencemag.org/cgi/content/full/302/5646/859>

A list of selected additional articles on the Science Web sites **related to this article** can be found at:

<http://www.sciencemag.org/cgi/content/full/302/5646/859#related-content>

This article **cites 20 articles**, 8 of which can be accessed for free:

<http://www.sciencemag.org/cgi/content/full/302/5646/859#otherarticles>

This article has been **cited by** 22 article(s) on the ISI Web of Science.

This article has been **cited by** 3 articles hosted by HighWire Press; see:

<http://www.sciencemag.org/cgi/content/full/302/5646/859#otherarticles>

This article appears in the following **subject collections**:

Oceanography

<http://www.sciencemag.org/cgi/collection/oceans>

Information about obtaining **reprints** of this article or about obtaining **permission to reproduce this article** in whole or in part can be found at:

<http://www.sciencemag.org/about/permissions.dtl>

- Sheet, C. J. Van der Veen, J. Oerlemans, Eds. (Reidel, Dordrecht, 1987).
29. I. Joughin, L. Padman, *Geophys. Res. Lett.* **30**, 1477 (2003).
30. E. Rignot, S. S. Jacobs, *Science* **296**, 2020 (2002).
31. K. Nicholls, personal communication.
32. J. K. Ridley, K. C. Partington, *International Journal of Remote Sensing* **9**, 601 (1988).
33. G. S. Brown, *IEEE Transactions of Antennas and Propagation* **25**, 67 (1977).
34. J. O. Speroni, W. C. Dragani, E. E. D'Onofrio, M. R. Drabble, C. A. Mazio, *Geoactas* **25**, 1 (2001).
35. N. Reeh, C. Mayer, O. B. Olesen, E. L. Christensen, H. H. Thomsen, *Ann. Glaciol.* **31**, 111 (2000).
36. A. Shepherd, N. R. Peacock, *J. Geophys. Res.* **108**, 3198 (2003).
37. C. S. M. Doake, *Ann. Glaciol.* **5**, 47 (1984).
38. J. G. Ferrigno *et al.*, AVHRR Antarctic Mosaic (USGS I-2560, 2001).
39. Supported by the United Kingdom Natural Environment Research Council Centre for Polar Observation and Modelling and Instituto Antártico Argentino. We thank the European Space Agency for ERS data and the British Antarctic Survey for access to the BEDMAP database.

We also thank J. Mansley, H. De Angelis, and G. Marshall for assistance with data collection and processing, and D. Vaughan and E. Morris for their valuable comments.

Supporting Online Material

www.sciencemag.org/cgi/content/full/302/5646/856/DC1
Table S1

29 July 2003; accepted 23 September 2003

Carbonate Deposition, Climate Stability, and Neoproterozoic Ice Ages

Andy J. Ridgwell,^{1*} Martin J. Kennedy,¹ Ken Caldeira²

The evolutionary success of planktic calcifiers during the Phanerozoic stabilized the climate system by introducing a new mechanism that acts to buffer ocean carbonate-ion concentration: the saturation-dependent preservation of carbonate in sea-floor sediments. Before this, buffering was primarily accomplished by adjustment of shallow-water carbonate deposition to balance oceanic inputs from weathering on land. Neoproterozoic ice ages of near-global extent and multimillion-year duration and the formation of distinctive sedimentary (cap) carbonates can thus be understood in terms of the greater sensitivity of the Precambrian carbon cycle to the loss of shallow-water environments and CO₂-climate feedback on ice-sheet growth.

The growth of continental-scale ice sheets extending to the tropics during the second half of the Neoproterozoic (1000 to 540 million years ago) (1) is now widely accepted in the geological community and has been of particular interest because of its close stratigraphic association with the first appearance of metazoans and the possibility that ice ages served as an environmental filter for animal evolution (2). The severity of these ice ages, which may record the coldest times in Earth history (3), implies that the Precambrian climate system must have operated very differently from today. This is supported by the ubiquitous occurrence of thin post-glacial "cap" carbonate units (4–7), apparent perturbations of the carbon cycle that did not recur in the Phanerozoic. To account for these observations, we focus on a first-order difference between the Precambrian and modern Earth systems and its implications for atmospheric CO₂: the absence of a well-developed deep-sea carbonate sink before the proliferation of calcareous plankton.

On the time scale of glaciations (~10⁴ to 10⁶ years), the balance between weathering of terrigenous rocks and the burial flux of calcium

carbonate (CaCO₃) in marine sediments exerts a key control on ocean carbonate chemistry (8), with this burial today divided roughly equally between deep-water (pelagic) and shallow-water (neritic) zones (9). The latter sink is of particular relevance in the context of ice ages, because the total neritic area available for CaCO₃ burial is highly sensitive to sea level, a consequence of the nonuniform distribution of the Earth's surface area with elevation (Fig. 1). The climatic relevance arises because any increase in the carbonate ion concentration ([CO₃²⁻]) at the ocean surface will induce lower atmospheric CO₂ (because the aqueous carbonate equilibrium, CO₂ + CO₃²⁻ + H₂O ↔ 2HCO₃⁻, is shifted to the right). This is the basis for the coral reef hypothesis for Quaternary glacial-interglacial CO₂ control (10–13), in which lowered sea level reduces available neritic area and CaCO₃ accumulation rates, driving higher [CO₃²⁻] and lower CO₂.

We have identified a fundamental difference between ancient and modern carbon cycles in the relative importance of the neritic carbonate sink that would make the impact of a coral reef-like effect much greater in the Precambrian. In the modern system, higher [CO₃²⁻] enhances the preservation of carbonate in deep-sea sediments; hence, a reduction in neritic carbonate deposition due to a fall in sea level can be compensated for by a greater burial flux in deep-sea sediments of CaCO₃ that originates from planktic calcifiers (9) (Fig. 1). This provides a strong negative (stabilizing) feed-

back on the modern carbon cycle, restricting oceanic [CO₃²⁻] variation and thus limiting the atmospheric response to sea level change.

The Neoproterozoic carbon cycle, by contrast, did not possess this stabilizing feedback, because before the advent of pelagic calcifiers in the Cambrian and the subsequent proliferation of coccolithophores and foraminifera during the Mesozoic (14), carbonate deposition would have been largely limited to neritic zones. The importance of the calcareous plankton that dominate carbonate deposition in the modern open ocean (9) is illustrated by the comparative rarity of deep-sea pelagic carbonate material in ophiolite suites older than ~300 million years (14). As neritic carbonate deposition was the dominant mechanism of CO₃²⁻ removal in the Precambrian ocean, it follows that atmospheric CO₂ would have been much more sensitive to sea level change. We explore the implications for the Neoproterozoic carbon cycle of sea level variation with the aid of a numerical model (15). This model calculates the evolution in atmospheric CO₂ that arises from a reduction in the area available for neritic carbonate deposition.

Although these observational and evolutionary arguments suggest a highly limited role for the deep-sea carbonate buffer in the Precambrian carbon cycle, Precambrian ocean chemistry would instead have been stabilized by the dependence of shallow-water carbonate deposition rates on [CO₃²⁻] (8). As oceanic [CO₃²⁻] (and saturation state, Ω) rises after a fall in sea level, the smaller area available for carbonate deposition is eventually compensated for by a higher precipitation rate per unit area. An analogous compensating increase in the neritic CaCO₃ precipitation rate may have occurred at the Cretaceous/Tertiary boundary after the extinction-driven reduction of pelagic carbonate productivity (8). The precipitation rate of carbonate minerals is expressed in the model as a proportionality with (Ω - 1)ⁿ (16), where Ω is defined as ([Ca²⁺] × [CO₃²⁻])/K_{sp} (where K_{sp} is a solubility constant). The parameter *n* is a measure of how strongly CaCO₃ precipitation rate responds to a change in ambient [CO₃²⁻] and thus of how effectively ocean chemistry and atmospheric CO₂ are buffered. Possible values range from ~1.0 for modern biological systems such as corals (17) to 1.9 ≤ *n* ≤ 2.8 for precipitation that occurs under entirely abiotic conditions (16). We therefore initially set *n* = 1.7 (8, 11). Because CaCO₃ precipitation dur-

¹Department of Earth Sciences, University of California–Riverside, Riverside, CA 92521, USA.

²Climate and Carbon Cycle Modeling Group, Lawrence Livermore National Laboratory, 7000 East Avenue, L-103, Livermore, CA 94550, USA.

*To whom correspondence should be addressed. E-mail: andyr@citrus.ucr.edu

REPORTS

ing the Neoproterozoic is dominantly associated with phototrophic (primarily cyanobacterial) communities (18), we assume it was restricted to the euphotic zone. The CaCO_3 sink strength is then proportional to the benthic area integrated over the uppermost ~ 100 m of ocean (A), giving a total deposition rate equal to $A \times k \times (\Omega - 1)^n$ (8, 11), where k is a scaling constant for precipitation rate per unit area.

We predicted a substantial drop in atmospheric CO_2 associated with the influence of incipient ice-sheet growth in the Neoproterozoic, which we simulated in the model by lowering sea level and recalculating ocean volume and available shallow-water area. In response to a prescribed 100-m sea level fall and a factor 3.2 reduction in depositional area (similar in magnitude to late Quaternary change), atmospheric CO_2 concentration dropped from 3400 to 2214 parts per million by volume (ppmv). Induced imbalances between volcanic CO_2 outgassing and silicate rock weathering then started to drive the system back toward initial steady state (Fig. 2, M1). This would have provided a peak radiative forcing of -2.3 W m^{-2} from direct CO_2 effects alone (19). However, configured with the modern carbonate depositional system, with planktic calcification that gives rise to a substantial deep-sea carbonate sink, the model exhibited relatively little CO_2 response (Fig. 2, M4) and a radiative forcing of just -0.4 W m^{-2} . This is because the reduction in the neritic sink is efficiently compensated for by increased carbonate preservation in deep-sea sediments. The success of calcareous plankton would have also reduced oceanic carbonate-ion concentrations, resulting in less inorganic carbon stored in the ocean and thus shorter time scales for ocean-carbonate chemistry to return to equilibrium. This stabilizing mechanism contrasts with the destabilizing role calcareous plankton could play if

Table 1. Model parameter values and initial ocean saturation state (Ω). Runs M1 through M4 assume modern topography and continental shelf area. Runs P1 through P4 assume an initial area of shallow-water depositional environments a factor of 3 larger (but with identical hypsometry at depths greater than 100 m). Run M4 (+ pelagic) has 50% of the global burial rate of 20 Tmol of $\text{CaCO}_3 \text{ year}^{-1}$ occurring as planktic carbonate in deep-sea sediments, whereas run P4 (+ erosion) has subaerially exposed carbonates eroding with a dissolution rate of 1.1 mol of $\text{CaCO}_3 \text{ m}^{-2} \text{ year}^{-1}$ (11).

Run	Ω	k	n	Notes
M1	6.5	0.05	1.7	
M2	4.3	0.12	1.7	
M3	3.1	0.25	1.7	
M4	3.1	0.12	1.7	+ pelagic
P1	6.5	0.06	1.0	
P2	6.5	0.017	1.7	
P3	6.5	0.004	2.5	
P4	6.5	0.017	1.7	+ erosion

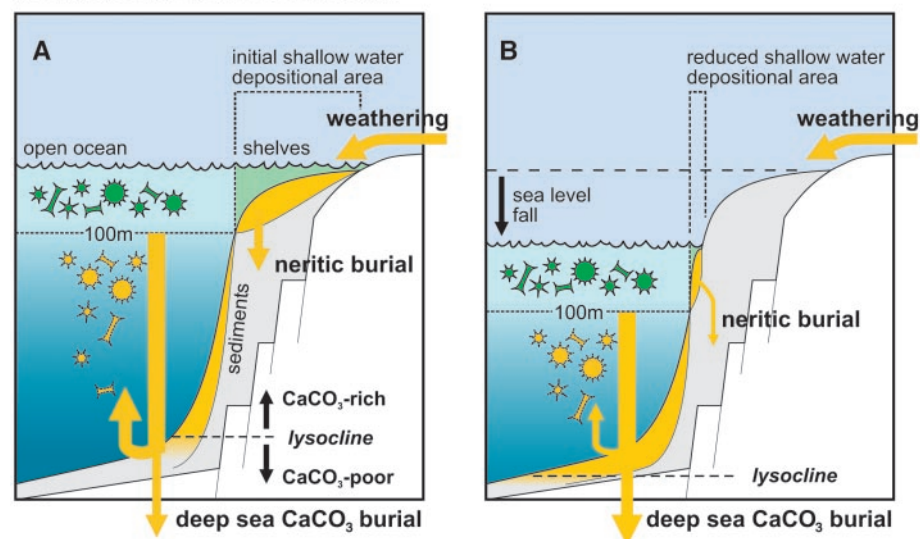
substantial amounts of deep-sea carbonate are returned to the atmosphere as metamorphic CO_2 at subduction zones (20).

The existence of broad regions of shallow intracratonic seas and rift basins in the late Neoproterozoic would have given a much greater contrast in neritic area with respect to sea level fall than assumed in the model runs with modern topography (Fig. 1). We tested this by increasing the initial area of flooded continental surface so that a 100-m sea level fall produced a factor ~ 10 reduction in neritic depositional area. Depending on the value of n in

the model (Table 1), atmospheric CO_2 could have fallen as low as 859 ppmv (Fig. 3A), equivalent to -7.4 W m^{-2} of climatic radiative forcing. The resulting cooling of the surface ocean would have drawn additional CO_2 from the atmosphere into the ocean. Furthermore, relations among CO_2 , surface temperature, ice volume, and sea level would have produced a positive feedback that would have amplified the initial direct effect, potentially leading to extreme global glaciation.

One unexpected aspect of our results is the slow recovery of the system through silicate

Modern system response to sea level fall



Potential initial system states in the Neoproterozoic

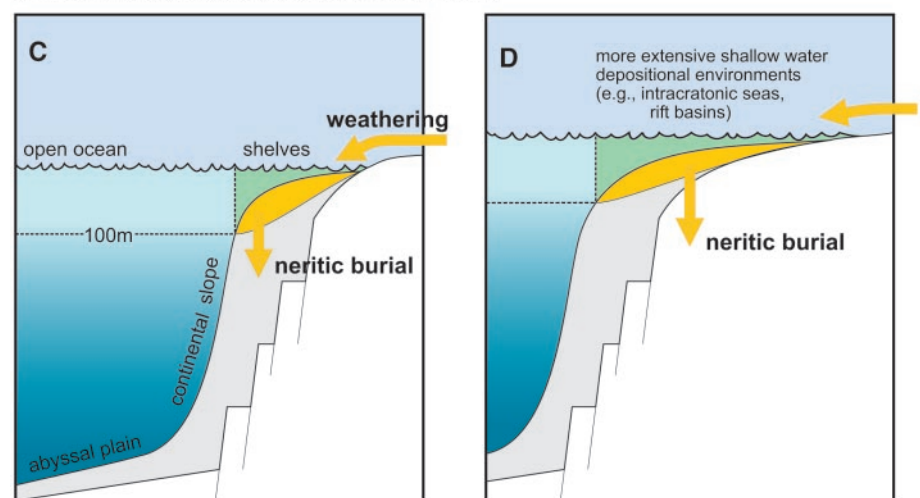


Fig. 1. Ancient and modern global carbonate cycling. (A and B) Schematic response of the modern system to a change in sea level: the coral reef mechanism (10–13). (A) High sea level stand at a steady state, with weathering input balanced by the burial of CaCO_3 in neritic and deep ocean environments. The CaCO_3 lysocline lies at a relatively shallow depth, with most planktic CaCO_3 to reach abyssal sediments dissolving. (B) Low sea level stand with reduced neritic area. Imbalance between sources and sinks of CO_3^{2-} results in increasing ocean saturation and decreasing atmospheric CO_2 . The preservation and burial of CaCO_3 in deep-sea sediments is enhanced, and the lysocline deepens until the loss of the neritic sink is compensated for. (C) The Precambrian system, lacking planktic calcifiers, with little burial of CaCO_3 in deep-sea sediments. Weathering input is balanced solely by shallow-water carbonate deposition. (D) The effect of a larger initial neritic area. A fall in sea level will now produce a much larger relative reduction in neritic area compared to that in (C), with a greater imbalance induced between sources and sinks of CO_3^{2-} .

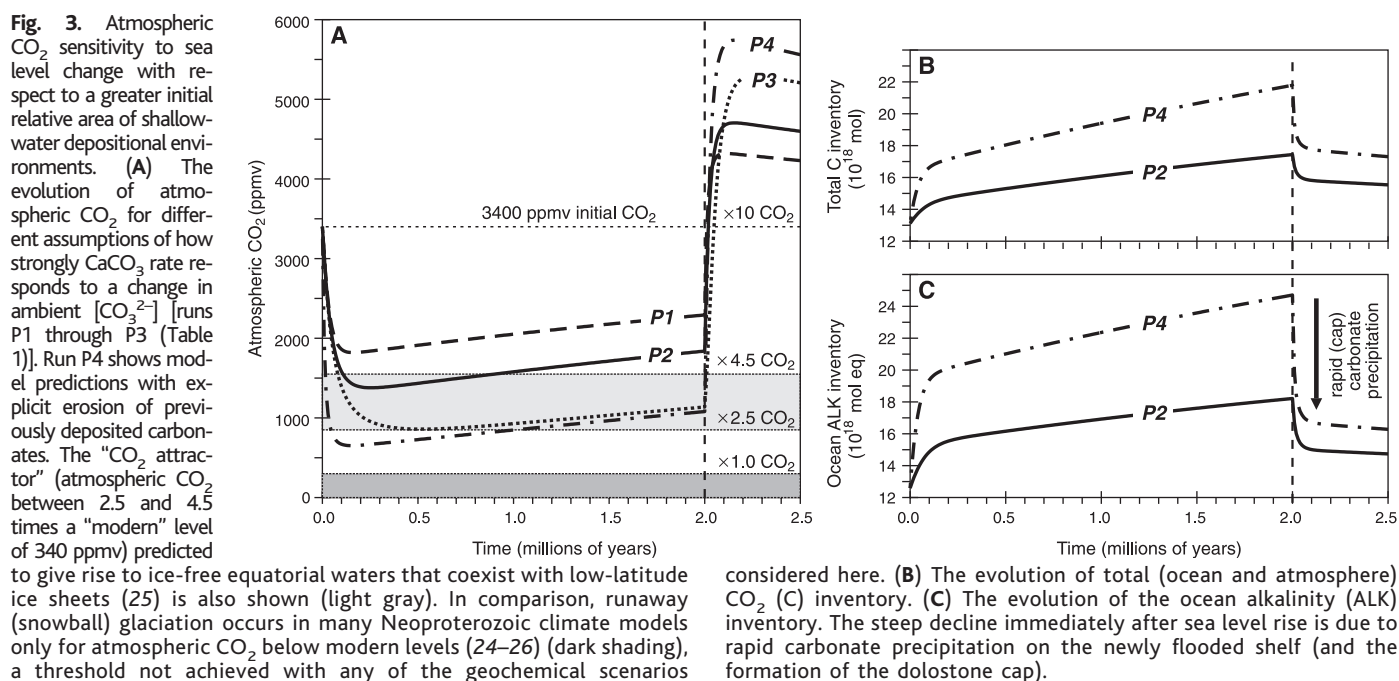
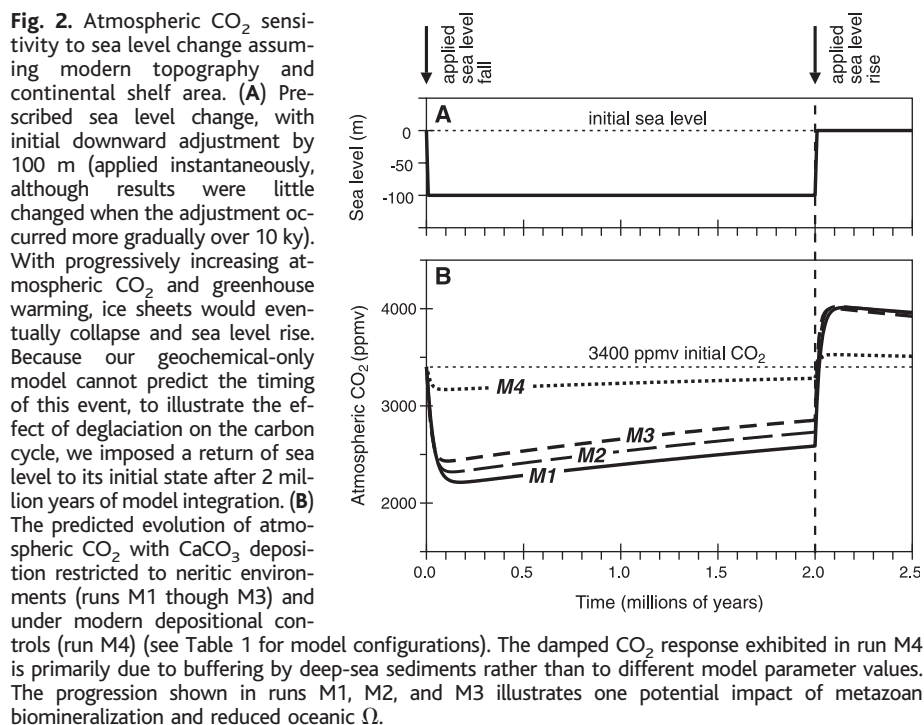
weathering (21): We find a time scale of more than 10^6 years [rather than $\sim 0.3 \times 10^6$ years (8)] for this negative feedback. This can be understood partly in terms of the extended residence time of CO_2 in a system with an initial inventory more than four times as large as the modern inventory, and rising to seven times after 2 million years (Fig. 3B). Interaction between the two negative feedbacks is also important, with the restoration of high atmospheric CO_2 through reduced weathering opposed by an induced decrease in neritic precipitation rate.

The result is that conditions of low CO_2 persist for millions of years.

The severity of Neoproterozoic glaciation can thus be understood in terms of the amplification of an initial perturbation through feedbacks involving the loss of neritic depositional environments. We hypothesize that cooling, incipient ice cap growth and initial sea level fall during times of rifting and intracratonic basin formation in the late Neoproterozoic initiated the neritic carbonate mechanism, which was then responsible for the severity and duration of these

ice ages. Supercontinent formation and fragmentation phases, which drive substantial changes in continental emergence and submergence (3), provide the necessary boundary conditions, consistent with the separation of episodes of Neoproterozoic glaciation on a tectonic time scale (5). This leaves aside the details of the mechanism(s) involved in driving incipient glaciation, although there is no lack of candidates (3–5).

The apparent ~ 1 -billion-year absence of severe glaciation before the Neoproterozoic (3) could be a result of insufficient topographic contrast to give the necessary reduction in neritic area upon sea level fall. That glaciation should have been comparatively mild during the Ordovician (3), a time also before the establishment of the modern mode of carbonate deposition but with evidence for extensive cratonic flooding, cannot be explained with the same reasoning. It may instead reflect sea level that lies above the inflection point in the distribution of continental area with altitude. A small sea level fall would then give rise to an increase rather than a decrease in neritic area, resulting in lower $[\text{CO}_3^{2-}]$ and higher CO_2 and damping rather than amplifying incipient glaciation. A second possibility involves the profound impact on biogeochemical cycling that the advent of carbonate secreting organisms (metazoans) must have had around the time of the Precambrian-Cambrian boundary (22). For instance, we find that a reduction in oceanic $[\text{CO}_3^{2-}]$ enhances the efficiency of neritic buffering and atmospheric CO_2 stability (Fig. 2B). Widespread biomineralization may also have resulted in the deep abyssal ocean becoming undersaturated. This, in conjunction with the evolution of the first pelagic calcifiers, could have enabled the development of an embry-



onic carbonate lysocline and helped prevent extreme Paleozoic glaciation.

One prediction of our hypothesis is that a relationship should exist between the thickness of post-glacial cap carbonate facies and excess alkalinity accumulated in the ocean during glaciation. We calculate that within 50 thousand years (ky) of sea level rise, 2.8×10^{18} to 7.1×10^{18} mole equivalents (mol eq) of accumulated alkalinity, equivalent to 1.4×10^{18} to 3.5×10^{18} mol CaCO_3 , was lost through precipitation, with more than 50% of the loss occurring in less than 10 ky (Fig. 3C). This is sufficient to form a carbonate layer that averages between 0.8 and 2.1 m thick and assumes a shelf area three times that of the present day (modern shelfal area being some 2.0×10^7 km²). This agrees well with typical cap (dolostone) thicknesses observed in shelfal settings of order meters (5, 7, 23). Thus, the occurrence of post-glacial cap carbonates is quantitatively consistent with a coral reef-like mechanism, with rapid deposition on newly flooded continental shelves taking place from a highly oversaturated ocean (6). Methane hydrate degradation (7) need only then add a portion of the required alkalinity.

The established framework for understanding Neoproterozoic glaciation envisages the onset of a completely frozen world through catastrophic ice-albedo feedback—the “snowball Earth” hypothesis (4, 5). An alternative climatic interpretation is of ice-free equatorial waters coexisting with low-latitude ice sheets (24–26). Although this has the advantage of providing a substantive refugium for multicellular life (2, 26), it has been rejected because of the need to account for the inferred longevity of glaciation and the occurrence of cap carbonates (5, 27). Our geochemical hypothesis answers both these deficiencies and predicts relatively stable atmospheric CO_2 consistent with the radiative forcing required by the open-water climate solution (25) (Fig. 3A).

The evolution of calcareous organisms marking the beginning of the Phanerozoic and the subsequent development of a responsive deep-sea carbonate sink drove a fundamental increase in the stability of the Earth’s carbon-climate system, limiting the extremity of glaciation possible. Before this, the weakly stabilizing neritic carbonate sink would have been the Achilles’ heel of the Precambrian climate system.

References and Notes

1. L. E. Sohl, N. Christie-Blick, D. V. Kent, *Geol. Soc. Am. Bull.* **111**, 1120 (1999).
2. B. Runnegar, *Nature* **405**, 403 (2000).
3. J. C. Crowell, *Pre-Mesozoic Ice Ages: Their Bearing on Understanding the Climate System*, *Geol. Soc. Am. Mem.* **192** (1999).
4. P. F. Hoffman, A. J. Kaufman, G. P. Halverson, D. P. Schrag, *Science* **281**, 1342 (1998).
5. P. F. Hoffman, D. P. Schrag, *Terra Nova* **14**, 129 (2002).
6. M. J. Kennedy, *J. Sediment. Res.* **66**, 1050 (1996).
7. M. J. Kennedy, N. Christie-Blick, L. E. Sohl, *Geology* **29**, 443 (2001).
8. K. Caldeira, M. R. Rampino, *Paleoceanography* **8**, 515 (1993).
9. J. D. Milliman, *Global Biogeochem. Cycles* **7**, 927 (1993).

10. W. H. Berger, *Naturwissenschaften* **69**, 87 (1982).
11. G. Munhoven, L. M. François, *J. Geophys. Res.* **101**, 21423 (1996).
12. A. J. Ridgwell, A. J. Watson, M. A. Maslin, J. O. Kaplan, *Paleoceanography*, doi:10.1029/2003PA000893, in press.
13. J. C. G. Walker, B. C. Opdyke, *Paleoceanography* **10**, 415 (1995).
14. S. K. Boss, B. H. Wilkinson, *J. Geol.* **99**, 497 (1991).
15. We used the PANDORA ocean carbon cycle model (28) coupled to a representation of the preservation and burial of CaCO_3 in deep-sea sediments (29) in a model configuration essentially the same as that used elsewhere (8, 11, 13). We provided long-term negative feedback by modifying weathering fluxes (73) of carbon (15 Tmol year⁻¹) and alkalinity (40 Tmol year⁻¹) according to the (pre-vascular plant) formulation of GEOCARB (27), while leaving volcanic CO_2 outgassing (5 Tmol year⁻¹) (13) constant. We made no additional reduction in global weathering rates because of glaciation, consistent with recent analysis of the late Quaternary glacial geochemical system (30). The presence or absence of planktic calcifiers was simulated by setting the surface ocean export ratio of CaCO_3 to organic matter in PANDORA to 0.2 or 0.0, respectively. We assumed the surface ocean was initially in equilibrium with atmospheric CO_2 at 3400 ppmv [sufficient to prevent the formation of ice sheets in climate models of the Neoproterozoic (24)] and with Ω at 6.5 with respect to aragonite (except where otherwise noted in Table 1), consistent with a Neoproterozoic ocean more highly saturated than at present (18, 23). Carbon and alkalinity inventories (Fig. 3, B and C) were thus uniquely determined (assuming present-day $[\text{Ca}^{2+}]$). The value of the CaCO_3 precipitation rate scaling constant, k , was set to achieve initial steady state (Table 1). Although variability in the carbonate carbon isotopic ratio is a distinctive feature of the Neoproterozoic geological record (4, 5, 7), without explicit representation of the controls on organic carbon burial, its interpretation cannot be advanced here.
16. S. J. Zhong, A. Mucci, *Geochim. Cosmochim. Acta* **57**, 1409 (1993).
17. N. Leclercq, J. P. Gattuso, J. Jaubert, *Global Change Biol.* **6**, 329 (2000).
18. R. Riding, *Sedimentology* **47**, 179 (2000).
19. V. Ramaswamy et al., in *Climate Change 2001: The Scientific Basis*, J. T. Houghton et al., Eds. (Contribution of Working Group I to the Third Assessment Report of the Intergovernmental Panel on Climate Change, Cambridge Univ. Press, New York, 2001), pp. 349–416.
20. K. Caldeira, *Geology* **19**, 204 (1991).
21. R. A. Berner, *Science* **249**, 1382 (1990).
22. R. A. Wood, J. P. Grotzinger, J. A. D. Dickson, *Science* **296**, 2383 (2002).
23. J. P. Grotzinger, A. H. Knoll, *Palaios* **10**, 578 (1995).
24. T. J. Crowley, W. T. Hyde, W. R. Peltier, *Geophys. Res. Lett.* **28**, 283 (2001).
25. S. K. Baum, T. J. Crowley, *Geophys. Res. Lett.* **28**, 583 (2001).
26. W. T. Hyde, T. J. Crowley, S. K. Baum, W. R. Peltier, *Nature* **405**, 425 (2000).
27. D. P. Schrag, P. F. Hoffman, *Nature* **409**, 306 (2001).
28. W. S. Broecker, T.-H. Peng, *Radiocarbon* **28**, 309 (1986).
29. A. J. Ridgwell, A. J. Watson, D. E. Archer, *Global Biogeochem. Cycles* **16**, 1071, doi:10.1029/2002GB001877 (2002).
30. I. W. Jones, G. Munhoven, M. Tranter, P. Huybrechts, M. J. Sharp, *Global Planet. Change* **33**, 139 (2002).
31. Supported by NSF and the Trusthouse Charitable Foundation (A.J.R.).

23 June 2003; accepted 26 September 2003

Origin and Migration of the Alpine Iceman

Wolfgang Müller,^{1*} Henry Fricke,² Alex N. Halliday,³ Malcolm T. McCulloch,¹ Jo-Anne Wartho⁴

The Alpine Iceman provides a unique window into the Neolithic-Copper Age of Europe. We compared the radiogenic (strontium and lead) and stable (oxygen and carbon) isotope composition of the Iceman’s teeth and bones, as well as ⁴⁰Ar/³⁹Ar mica ages from his intestine, to local geology and hydrology, and we inferred his habitat and range from childhood to adult life. The Iceman’s origin can be restricted to a few valleys within ~60 kilometers south(east) of the discovery site. His migration during adulthood is indicated by contrasting isotopic compositions of enamel, bones, and intestinal content. This demonstrates that the Alpine valleys of central Europe were permanently inhabited during the terminal Neolithic.

A well-preserved human mummy, the “Iceman,” was recovered from a glacier located at the main Alpine watershed between Italy and Austria in 1991. The Iceman was ~46 years old and lived ~5200 years ago. Both the mummy and its associated equipment

provided unprecedented insights into daily life during the late Neolithic-Copper Age of central Europe (1–4). One of the remaining questions regarding the Iceman is his place of origin. Molecular genetic analyses suggest that the Iceman’s mitochondrial DNA closely resembles that of central and northern Europeans, including people from the Alpine region (5). Poor preservation prevented the recovery of nuclear DNA, thereby restricting better spatial resolution of his origin (5, 6). For the Iceman’s late adulthood, his southern origin in present-day northern Italy has been deduced from the pollen and moss contents of his intestine (7, 8). The lack of pottery among his

¹Research School of Earth Sciences, The Australian National University, Canberra, ACT 0200, Australia. ²Department of Geology, Colorado College, 14 East Cache La Poudre Street, Colorado Springs, CO 80903, USA. ³Department of Earth Sciences, ETH Zürich, CH-8092 Zürich, Switzerland. ⁴Department of Applied Geology, Curtin University of Technology, GPO Box U1987, Perth, WA 6845, Australia.

*To whom correspondence should be addressed. E-mail: wolfgang.mueller@anu.edu.au